Identification of reaction mechanism for anodic dissolution of metals using Electrochemical Impedance Spectroscopy

Jeevan Maddala, S. Krishnaraj, Vinod Kumar, and S. Ramanathan[*]

Department of Chemical Engineering, Indian Institute of Technology-Madras, Chennai 600 036, India.

Abstract: Electrochemical Impedance Spectroscopy (EIS) is a sensitive technique for determining the mechanistic pathway of an electrochemical reaction. In particular, the low frequency behavior of the impedance at various over potentials can help differentiate between very similar mechanisms. Nine different mechanisms related to anodic dissolution of metals are simulated and the EIS patterns that are expected for these mechanisms are identified. This library of patterns reported here will help in eliminating certain mechanisms and identifying mechanisms with the least number of parameters that can be applied for modeling experimental EIS data.

Key words: Electrochemical Impedance Spectroscopy; EIS; reaction mechanism; complex-plane plot; anodic dissolution.

[*] srinivar@iitm.ac.in

Introduction

EIS has been widely applied for studying the characteristics of electrodes and electrochemical reactions [1-3]. In this technique a small ac voltage perturbation is applied to the electrochemical system and the resulting current is measured, from which the impedance can be calculated. The impedance is measured at various frequencies and is typically plotted as the negative of the Imaginary component vs Real component (complex-plane plot) or as magnitude vs logarithm of frequency and phase vs logarithm of frequency (Bode plots). Both complex-plane plots and Bode plots provide the same information in different perspectives. In simple systems, the impedance plots are used to identify the solution resistance, the double layer capacitance and the diffusion resistance known as Warburg impedance. This is normally modeled by an electronic circuit with a resistance, capacitance and Warburg impedance (Fig.1).

Impedance measurements of many reacting systems yield complex-plane plots (and Bode plots) with characteristic features that are very different from those of non-reacting systems. In some simple cases, the data can be modeled with adding few elements such as capacitance or inductance or constant phase elements (CPE) [4]. These electrical equivalent circuits (EEC) can provide a reasonable fit for some of the data and have been used for describing the impedance data of some systems [4-8]. However in many cases EECs do not provide sufficient insight into the reaction pathway. The reaction mechanism analysis (RMA) [9, 10] is a method wherein a mechanism is proposed and the impedance data is simulated for that mechanism. The simulated data is compared with the experimental data, particularly for the features in the plots. A mechanism that leads to features or patterns that are similar to the experimental data is chosen

and the other mechanisms are rejected. The parameters can be estimated using optimization techniques [11,12] or by trial and error [10].

It is possible that more than one mechanism can lead to similar results [13]. If additional data is available (e.g. from non-electrochemical experiments), some of the candidate mechanisms can be eliminated. Otherwise, ideally the mechanism that can fit the data with the least number of parameters should be chosen. In order to choose the best candidate mechanisms, a library of patterns for corresponding to various mechanisms is necessary [13]. For some of the reactions, the equivalent circuits representing the reactions have been established and the relationship between the circuit element values and the reaction parameters have also been determined [14-16]. In some cases, the system may exhibit a loop that can be modeled with inductors. However, it is not easy to rationalize modeling the data with an inductor because there is no magnetic field associated with the adsorption-reaction process [16]. Besides, the inductances required for fitting the data are also very high [16] and hence the behavior is more appropriately called as negative capacitance [14, 16]. Systems showing negative capacitance loop have been analyzed in relation to a two step electron transfer mechanism and parameter phase plots which map out zones where different behavior such as positive or negative capacitive arcs occur have been presented [15]. For metals in passive and transpassive regions, Armstrong et al. [17] determined the shape of the impedance curves in certain limiting conditions of relaxation times and showed that positive or negative capacitance or a combination of negative resistance and negative capacitance may be possible. The impedance may be from the geometric capacitance of the film or from the film-solution interface. Second order effects can be observed in systems with two adsorbed species and the evolution of the impedance arcs with increase in overpotential has also been

characterized [18]. The diagrams indicate the presence of positive and negative capacitance loops occurring in various sequences depending on the reaction parameters and the double layer capacitances. In another report for a specific second order system, the impedance spectra were simulated to understand certain unusual patterns such as negative resistances and capacitances [19]. Some systems exhibiting resonance (sharp peaks in the impedance magnitude vs frequency plots) show unusual spectra and some of the patterns exhibited by these systems have also been reported [20].

More complicated patterns have been observed experimentally and modeled in some cases with specific reaction mechanisms. However, to the authors' knowledge, there is no set of library of patterns for different mechanisms reported in the literature. In this report, a set of nine mechanisms for anodic dissolution of metals are analyzed systematically and the EIS patterns arising from those mechanisms are reported. The patterns are obtained by numerical simulation and in two cases they are also compared with analytical results.

Simulation:

Various mechanisms that are analyzed in this report are given in Fig 2.The development of equations for impedance for different mechanisms have been reported in the literature [12, 21-24] and two brief examples are given below. The following assumptions are utilized in the derivation.

      1. The double layer capacitance is a constant throughout the voltage range simulated

      2. The perturbation is linear and the higher order terms can be neglected. This is applicable as long as the applied ac voltage for EIS studies is a few mV.

3. The kinetic parameters depend exponentially on the voltage, showing a behavior similar to that of Tafel constants.

4. The forward reaction will have a non-negative exponent and the reverse reaction will have a non-positive exponent and

5. The adsorption of the charged species follows the Langmuir isotherm model. Thus the surface coverage is restricted to unity.

A set of parameter values is chosen for the simulation as shown in Table 1. The parameter ranges were chosen based on the data reported in the literature. The kinetic parameters were also constrained based on the estimated impedance values. If the kinetic parameters are very small, then the impedance values will be in the order of giga ohms. Experimentally, measuring very high impedance in electrochemical systems accurately, particularly for low frequencies, will be difficult. On the other hand, very large values for the kinetic parameters will lead to extremely low impedance, again leading to difficulties in measurements. Thus the kinetic parameters ranges are chosen to represent typical systems. The frequency range is based on what is available in commercial frequency response analyzers (FRA) that are commonly used. The impedance data were simulated for each parameter combination and all the unique shapes possible for a given mechanism were identified.

The notation used for identifying the patterns is as follows. If both the real and imaginary parts of the impedance increase with frequency, the shape is denoted as A and if the real part increases but the imaginary part decreases, the shape is denoted as B (Fig 3. a and b) Similarly, if the real part decreases but the imaginary part increases, the shape is denoted as C, while the shape where

both decrease with frequency is denoted as D (Fig 3.c and d). For example, for a simple

capacitance curve (Fig 3.e), the shape is first D at the lowest frequency and then C at the higher

frequencies. The overall shape of the curve is DC. A double capacitance curve (Fig 3.g) has a

shape DCDC and a curve with negative capacitance behavior (Fig 3.h) has a shape of ABDC. It

is to be noted that in this work the shape is determined when the frequency is increased from low

to high value. Many electrochemical instruments report data with frequency in the descending

order. When comparing the shape of experimental data and simulated data, this fact has to be

accounted for. The figures show sample results, with emphasis on the shape rather than the

magnitude. EIS data with larger or smaller magnitude can be modeled by changing the parameter

values and the frequencies at which various arcs appear will also change with the parameter

values.

Some of the mechanisms lead to more than a hundred patterns. In those cases, only few select

cases are reported based on the number of times a pattern was observed and resemblance to data

in the published literature. It is to be noted that whenever the shape is reported as possible, a sub-

section of the shape is also possible. i.e. if DCDC is a possible shape, then DCD or CDC , DC,

CD, D and C are the sub-section shapes that may be observed for a system.

Results and Discussion:

Fig. 3 shows various impedance patterns that are possible with the mechanisms investigated in

this report and table 2 summarizes the mechanisms and the corresponding patterns. Here, M

represents the metal atoms, M^+_{ads} the adsorbed metal ion and M^+_{sol} the metal ion in solution.

Mechanism 1 involves a simple metal ion adsorbed on the metal as an intermediate species in the dissolution. The first step corresponds to the charge transfer reaction, while the second step is a simple dissolution. The mass balance for the adsorbed species yields

$$\tau \frac{d\theta}{dt} = k_1 (1-\theta) - k_2 \theta ,$$

where τ corresponds to the number of sites at monolayer coverage and θ is the surface coverage of the adsorbed species. In this equation, k_1 is the rate constant for the first step given by the formula

$$k_1 = k_{10} e^{b_1 V} .$$

Here, the b_1 is given by the equation

$$b = \pm \frac{\alpha F}{RT} ,$$

where α is the transfer coefficient with a value between 0 and 1, F is the Faraday constant, R is the universal gas constant and T is the temperature. For anodic dissolution, the positive sign is used for the oxidation and the negative sign for the reduction reaction respectively. The other rate constants are also given by similar formulas. Under steady state conditions, the surface coverage is given by

$$\theta_{ss} = \frac{k_1}{k_1 + k_2} .$$

The unsteady state equation, under small voltage perturbation gives rise to

$$\frac{d\theta}{dV} = \frac{(b_1 - b_2) k_2 \theta_{ss}}{k_1 + k_2 + j\omega\tau}$$

where j is the square root of -1 and ω is the angular frequency related to the frequency by the formula $\omega = 2\pi f$.

The unsteady state current is given by

$$i = Fk_1(1-\theta).$$

Differentiating the above equation with respect to potential and retaining only the first order terms, we get the following expression for $Z_{F,m/s}$, the Faradaic impedance at the metal solution interface:

$$\frac{di}{dV} = \frac{1}{Z_{F,m/s}} = (R_t)^{-1} - Fk_1 \frac{d\theta}{dV},$$

Where

$$(R_t)^{-1} = Fb_1k_1(1-\theta_{SS}).$$

The overall impedance of the system is given by

$$Z = R_{sol} + \frac{1}{Z_{F,m/s} + j\omega C_{dl}}$$

where R_{sol} is the solution resistance and C_{dl} is the double layer capacitance.

If b_1 is greater than b_2, then $\frac{d\theta}{dV}$ will be positive and increasing frequency (ω) will lower the magnitude of $\frac{d\theta}{dV}$, which will decrease the magnitude of $Z_{F,m/s}$. Thus the overall impedance will decrease with increasing frequency and $Z_{F,m/s}$ and C_{dl} lead to a double capacitance loop for these systems (Fig 3.g). The double capacitance loop has been observed for copper dissolution in sulfate solutions [24] at all the measured potentials and for other systems such as Ta dissolution in HF[4], Fe in sulfuric acid [9], Fe-Cr alloy in sulfate media [21], and Cu in nitric acid [23] although in conjunction with other shapes at different over potentials.

On the other hand, if the exponent b_2 is greater than b_1, then an increase in voltage would correspond to decrease in the surface coverage of the adsorbed species. In this case, increase in the frequency of applied perturbation would increase the impedance (Fig 3.h). While this would indicate that an equivalent circuit with inductor can be used to model this spectra, a negative capacitor is a more appropriate choice as indicated before. The negative capacitance loop has been observed experimentally, e.g. for the dissolution of chromium in acidic sulfate solution [25]. If b_1 and b_2 are equal, then the surface coverage is independent of over-potential and the system does not exhibit any additional loop (Fig 3.e). While a system may exhibit any one of the three possibilities, the overall shape of the impedance data in complex-plane plot format will not change with over potential for this mechanism. Hence with this mechanism, it is not possible to model a system which shows two positive capacitance loops at some over potentials and one negative capacitance behavior at some other over potentials. The simulation results (Table 2) match with the predictions of the analytical results. However, it must be noted that near equilibrium (i.e. at very low overpotentials), mechanism 1 will be reversible and will turn into mechanism 2 and hence practically, the ability to differentiate between mechanism 1 and 2 will be determined by the overpotentials at which the spectra are acquired. This result also enables one to obtain bounds for some of the parameters. For example, if a systems shows only negative capacitance behavior for many over potentials, then mechanism 1 can be chosen as a suitable candidate and the constraint $b_2 > b_1$ can be added to the data fit algorithm for quicker optimization.

In mechanism 1, making the first step reversible leads to mechanism 2 and the corresponding complex-plane plots are similar to those exhibited by mechanism 1. However, depending on the

9

value of the parameters, the system may exhibit two capacitance loops at low over potentials and

show negative capacitance behavior at higher over potentials. The relevant equations are

$$\frac{d\theta}{dV} = \frac{\left[(b_1 - b_{-1})k_{-1} + (b_1 - b_2)k_2\right]\theta_{ss}}{k_1 + k_{-1} + k_2 + j\omega\tau}$$

and

$$\frac{di}{dV} = \frac{1}{Z_{F,m/s}} = (R_t)^{-1} - F(k_1 + k_{-1})\frac{d\theta}{dV}$$

where

$$(R_t)^{-1} = F\left[b_1 k_1(1-\theta_{ss}) - b_{-1}k_{-1}\theta_{ss}\right].$$

It is to be noted that b_{-1} is constrained to have only zero or negative values. Like mechanism 1,

this mechanism can also lead to double capacitance loops if b_1 is greater than b_2. However if b_1 is

less than b_2, it may either (a) lead to negative capacitance behavior at all over potentials or (b) to

double capacitance loops at lower over potentials and negative capacitance behavior at higher

over potentials. The latter case would be observed if k_2 is small and k_{-1} is large. The sign of

$\frac{d\theta}{dV}$ would change from positive to negative with increase in over potential and the behavior

would change from that of double capacitance to negative capacitance. Here again the simulation

results match with the predictions of analytical results.

Dissolution by catalytic mechanism (mechanism 3) yields impedance data which shows, in

addition to the patterns shown is Fig 3.g and 3.h, another pattern that typically cannot be

modeled with capacitors with positive parameter values (Fig 3.i). This pattern has also been

reported for dissolution of Fe-Cr alloy in acid [21]. All these patterns are observed for various

combinations of b_1 and b_2. The catalytic mechanism is described as the reaction between an

empty site (film or metal site) and an adsorbed species and has been utilized to explain the dissolution of iron in sulfuric media [9] and in phosphoric acid [26]. The adsorbed species is denoted by M^{+*} to indicate that it is a metal ion associated with the anion in the solution. Since the net reaction does not consume the adsorbed species, it is called catalytic mechanism. It is to be noted that the first reaction has to be reversible or else the surface coverage will always be unity. For the second step, which is a second order catalytic reaction, the current density at the film/solution interface has been reported as

$$i = F\,k_2\theta\,,$$

whereas the correct equation would be

$$i = Fk_2\theta(1-\theta)\,,$$

since the presence of a vacant site (i.e. without any adsorbed ion) adjacent to the M^{+*} species is necessary for the reaction to proceed.

For unsteady state conditions, the mass balance leads to

$$\tau\frac{d\theta}{dt} = k_1(1-\theta) - k_{-1}\theta$$

since the second catalytic reaction does not lead to any change in the surface coverage of the adsorbed species. The steady state coverage is

$$\theta_{ss} = \frac{k_1}{k_1 + k_{-1}}$$

and the total current density is

$$i = F\left[k_1\left(1-\theta\right) - k_{-1}\theta + k_2\theta(1-\theta)\right].$$

This leads to the following equation for the Faradaic impedance at the film/solution interface.

$$\left(Z_{F,f/s}\right)^{-1} = \left(R_t\right)^{-1} + F(k_1 + k_{-1} - k_2(1 - 2\theta))\frac{d\theta}{dV},$$

where

$$\left(R_t\right)^{-1} = F((b_1 - b_{-1})k_{-1}\theta + b_2 \, k_2 \, \theta(1 - \theta))$$

and

$$\frac{d\theta}{dV} = \frac{(b_1 - b_{-1})k_{-1}\theta}{k_1 + k_{-1} + j\omega\tau}.$$

The total impedance is given by

$$Z = \frac{1}{\left(Z_{F,m/s}\right)^{-1} + j\,\omega C_{dl}}.$$

The equations that were used the literature lead to slightly different impedance equations. However, for a given set of parameters, the difference between the reported equations and the corrected equations is very small. Catalytic mechanism can also describe reactions which show double capacitance at one over potential and negative capacitance loop at another (either higher or lower) over potential regardless of whether b_1 is greater or less than or equal to b_2. This is unlike mechanism 2 which can fit only the cases where negative capacitance loop occurs at higher over potentials. The new shape BACDC however will occur only at higher over potentials and the system will not show double capacitance or negative capacitance behavior after the BACDC shape occurs.

A second order reaction between two adsorbed species leading to either two (mechanism 4) or one (mechanism 5) dissolved ion results in the same set of equations with the condition that k_{20} for mechanism 5 is equal to half the k_{20} for mechanism 4. Thus it is not possible to distinguish between the two mechanisms with pattern matching of EIS data alone. For these mechanisms,

when b_1 is greater than b_2, a double capacitance loop and BACDC patterns are possible regardless of over potential. When b_1 and b_2 are equal, only the simple DC pattern is possible, while the case of b_1 less than b_2 leads to negative capacitance loop. A slightly different catalytic pathway, where a vacant site participates in the reaction but does not get consumed is shown in mechanism 6. If k_1 is less than k_2, then the coverage of the adsorbed species will be less than 1. Otherwise, the steady state coverage will be unity and it will not depend on the voltage. The EIS data for such a case will be similar to those shown in Fig 1. In this simulation, only the cases where k_1 is less than k_2 are considered. This leads to patterns similar to those given by mechanism 3. However, when b_1 is greater than b_2, only a double capacitance loop followed by BACDC pattern at higher voltages are possible, while b_1 less than b_2 leads to a negative capacitance loop only. The case of b_1 equals b_2 yields the simple DC pattern.

Mechanism 7 is similar to mechanism 1 except that the second step also involves a charge transfer. Again for b_1 equal to b_2, the DC pattern would be observed. However, for b_1 either greater than or less than b_2, a negative capacitance loop at lower over potentials and double capacitance loop at higher over potentials are possible. This is just the inverse of the behavior that would be exhibited by systems following mechanism 2. Mechanism 8 is the extension of mechanism 7 with a reversible first step. In this case if b_1 is equal to b_2, a double capacitance loop may be observed at lower over potentials and a negative capacitance loop at higher over potentials. For b_1 not equal to b_2, both double capacitance and negative capacitance loops may be observed in any combination for various over potentials.

A series reaction (mechanism 9) applicable for situations where the final ionic species has valence more than one leads to a large variety of patterns. Apart from the patterns exhibited by the mechanisms investigated earlier in this report, a negative capacitance with double capacitance loop ABDCDC (Fig 3. m) , a triple capacitance loop DCDCDC (Fig 3. l) , a capacitance-negative capacitance- capacitance loop DCABDC (Fig 3.n) and double negative capacitance with capacitance loop ABABDC (Fig 3.k) are interesting patterns that are possible for this mechanism. The triple capacitance loop has been observed for dissolution of iron-chromium alloy [20]. The capacitance-negative capacitance-capacitance pattern has been experimentally observed for dissolution of iron in sulfuric media[9], Al in KOH [10], Cu in nitric acid [23] and Ni in sulfuric media[27]. The last pattern ABABDC has also been reported for dissolution of iron in sulfuric media [9] while a sub-shape BABDC (Fig 3.j) has been observed for dissolution of Ta in HF [4] and Cu in nitric acid [23]. The number of combinations of the patterns that may be observed for various over potentials is very high and hence not all of them are reported. It is worth noting that the number of parameters that can be fit is the same for mechanism 2, 3, 8 and 9. While mechanism 2 and 3 are applicable for species with single or multivalent ions, mechanism 8 and 9 are applicable only for multivalent ions. Thus it is likely that whenever a data is found to be described by mechanism 8, it is also described equally well by mechanism 9. However, the converse is not always true since there are some unique patterns such as triple capacitance loop which may be observed for reactions following the mechanism 9 that cannot be described by mechanism 8.

When various models are used to fit the data, it is preferable to use the model with the least number of parameters first. For example, if the EIS data shows negative capacitance loops for

various over potentials, both mechanism 1 and mechanism 2 are suitable initial candidates. However, mechanism 1 has less number of parameters and should be the preferred choice. The patterns provided here will be of use in eliminating some reaction mechanisms for a given set of impedance data. Simulating the EIS patterns for other mechanisms will lead to a more comprehensive library of patterns that can be used to identify even more complicated mechanisms. The impedance behavior of the system containing a passivating film has been described by the point defect model [28]. The possible EIS patterns for reactions involving passivation film need to be catalogued for a better understanding of the common metal-aqueous solution systems. While it is relatively easy to simulate the impedance spectra for a specific reaction and parameter set, the reverse problem of identifying the mechanism from the spectra is made difficult by the nonlinear equations involved. Since the ranges of the parameters are restricted and the impedance spectra are simulated only for a limited number of values, it is possible that patterns other than those listed in this report may exist for the above mechanisms. Nevertheless, since the parameter set and the frequency range are chosen based on the reported data and current instruments' capabilities, it is believed that the simulation results reported here provide a fairly complete set of library of patterns for these mechanisms.

Summary:

Nine different reaction mechanisms for anodic dissolution of metals have been simulated and a library of possible EIS patterns corresponding to these mechanisms for a typical range of parameters and frequencies has been generated. For two mechanisms, the simulation results are compared with analytical predictions and they are found to match well. It is shown that some of the mechanisms cannot be distinguished based on EIS data alone, while in other cases, clear

differentiation is possible. The library of patterns will enable screening candidate mechanisms quickly. In some cases, a bound for some of the parameters can also be obtained based on the patterns observed. Even if the experimentally observed patterns are possible for a certain mechanism, the dependence of pattern shape on the over potentials can also help in eliminating some candidate mechanisms and thus subtle differences in the reaction mechanisms can be determined. Identification of EIS patterns for more complicated mechanisms and mechanisms involving film formation will lead to a more comprehensive library of patterns that can be used for identifying reaction pathways.

References:

1. P. Marcus, Corrosion Mechanisms in theory and practice, Second ed., Marcel Dekker, New York, 2002.

2. E. Barsoukov, J.R. Macdonald, Impedance Spectroscopy, Second. Ed., John Wiley and Sons, New Jersey 2005.

3. M. Orazem, B. Tribollet, Electrochemical Impedance Spectroscopy, John Wiley and Sons, New Jersey, 2008

4. S. Sapra, H. Li, Z. Wang I.I. Suni, J. Electrochem. Soc. 152(6) (2005) B193.

5. J.R. Macdonald, Electrochim. Acta 35(10) (1990) 1483.

6. P.Agarwal, M. E. Orazem, M.H. Garia-Rubio, J. Electrochem. Soc. 139(7) (1992) 1917.

7. M. Bojinov, Electrochim. Acta, 42 (23-24) (1997) 3489.

8. J. Lu, J. E. Garland, C. M. Pettit S. V. Babu, D. Roy J. Electrochem. Soc. 151(10) (2004) G717.

9. B.Bechet, I. Epelboin, M. Keddam, J. Electronanal. Chem. 76 (1977) 129.

10. I. Epelboin, M. Joussellin, R. Wiart, J. Electroanal. Chem. 119 (1981) 61.

11. O. Pensado, M. U. Macdonald, D. D. Macdonald, J. Electrochem. Soc. 148 (10) (2001) B386.

12. D.D. Macdonald, S. Real, S.I. Smedley, M. Urquidi-Macdonald, J. Electrochem. Soc. (1988) 135(10) 2410.

13. D.D. Macdonald, Electrochim. Acta 51 (2006) 1376.

14. D.A. Harrington, P. van den Driessch, J. Electroanal. Chem. 567 (2004) 153.

15. J.P. Diard, B. Le Gorrec, C. Montella, J. Electroanal. Chem. 326 (1992) 13.

16. D.R. Franceschetti, J.R. Macdonald, J. Electroanal. Chem. 82 (1977) 271.

17. R.D. Armstrong, K. Edmondson, Electrochim. Acta 18 (1973) 937.

18. J. P. Diard, B. Le Gorrec, C. Montella, C. Montero-Ocampo, J. Electroanal. Chem. 352 (1993) 1.

19. A. Sadkowski, Solid State Ionics, 176 (2005) 1987.

20. A. Sadkowski, J. Electroanal. Chem. 573 (2004) 241.

21. M. Keddam, O.R. Mattos, H. Takenouti, Electrochim. Acta, 31(9) (1986) 1147.

22. M. Keddam, O.R. Mattos, H. Takenouti, Electrochim. Acta, 31(9) (1986) 1159.

23. W-J. Lee, Mater. Sci. Engg. A 348 (2003) 217.

24. D.K.Y. Wong, B.A.W. Coller, D.R. Macfarlane, Electrochim. Acta 38(14) (1993) 2121.

25. M. Bojinov, G. Fabricius, T. laitinen, T. Saario, J. Electrochem. Soc. 149(6) (1998) 2043.

26. M. Bojinov, I. Betova, G.Fabricius, T. Laitinen, R. Raicheff, J. Electroanal. Chem. 475 (1999) 58.

27. J. Gregori J.J. Garcia-Jareno, D. Gimenez-Romero, F. Vicente, J. Solid-State Electrochem. 9 (2005) 83.

28. C.Y. Chao, L.F. Lin, D.D. Macdonald, J. Electrochem. Soc. 129(9) (1982) 1874.

Figure and Table Captions

Figure 1. Electrical Equivalent Circuit (EEC) . R_{sol} - solution resistance, R_{ct}- Charge Transfer resistance, C_{dl}- double layer capacitance, W -Warburg Impedance

Figure 2. Various mechanisms that are analyzed

Figure 3. EIS patterns in complex-plane plot format. Arrow indicates the direction of increasing frequency

Table 1. Parameter ranges chosen for simulation. The increment type "G" represents geometric progression and "A" represents arithmetic progression.

Table 2. Various mechanisms and the EIS patterns generated. *Some of the additional patterns observed for mechanism 9 are BABDC, DCDCDC, ABDCDC and DCABDC

Figure 1.

Figure 2.

Mechanims 1: $M \xrightarrow{K_1} M^+_{ads} + e^- \xrightarrow{K_2} M^+_{sol}$

Mechanism 2: $M \underset{K_{-1}}{\overset{K_1}{\rightleftharpoons}} M^+_{ads} + e^- \xrightarrow{K_2} M^+_{sol}$

Mechanism 3: $M \underset{K_{-1}}{\overset{K_1}{\rightleftharpoons}} M^{+*}_{ads} + e^-$

$\qquad\qquad M^{+*}_{ads} + M \xrightarrow{K_2} M^{+*}_{ads} + M^+_{sol} + e^-$

Mechanism 4: $M \xrightarrow{K_1} M^{+*}_{ads} + e^-$

$\qquad\qquad M^{+*}_{ads} + M^{+*}_{ads} \xrightarrow{K_2} M^+_{sol} + M^+_{sol}$

Mechanism 5: $M \xrightarrow{K_1} M^{+*}_{ads} + e^-$

$\qquad\qquad M^{+*}_{ads} + M^{+*}_{ads} \xrightarrow{K_2} M^{+*}_{ads} + M^+_{sol}$

Mechanism 6: $M \xrightarrow{K_1} M^+_{ads} + e^-$

$\qquad\qquad M^+_{ads} + M \xrightarrow{K_2} M + M^+_{sol}$

Mechanism 7: $M \xrightarrow{K_1} M^+_{ads} + e^- \xrightarrow{K_2} M^{2+}_{sol} + e^-$

Mechanism 8: $M \underset{K_{-1}}{\overset{K_1}{\rightleftharpoons}} M^+_{ads} + e^- \xrightarrow{K_2} M^{2+}_{sol} + e^-$

Mechanism 9: $M \xrightarrow{K_1} M^+_{ads} + e^- \xrightarrow{K_2} M^{2+}_{ads} + e^- \xrightarrow{K_3} M^{2+}_{sol}$

21

Figure 3.

(a)

(b)

(c)

(d)

(e)

(f)

(g)

(h)

(i)

(j)

(k)

(l)

(m)

(n)

22
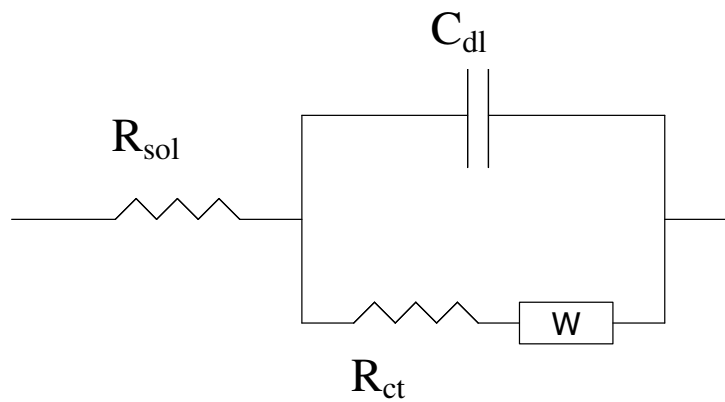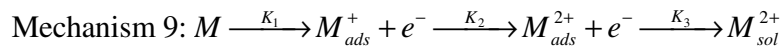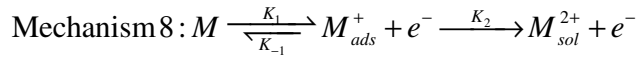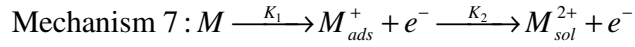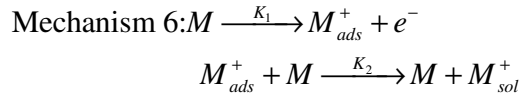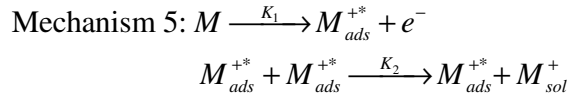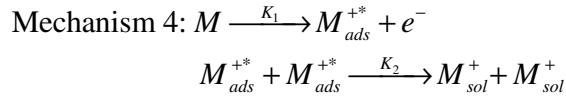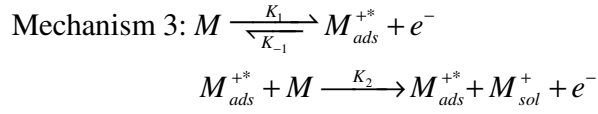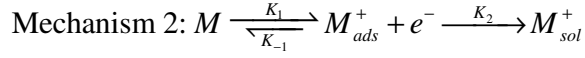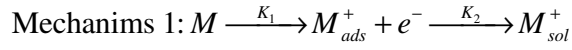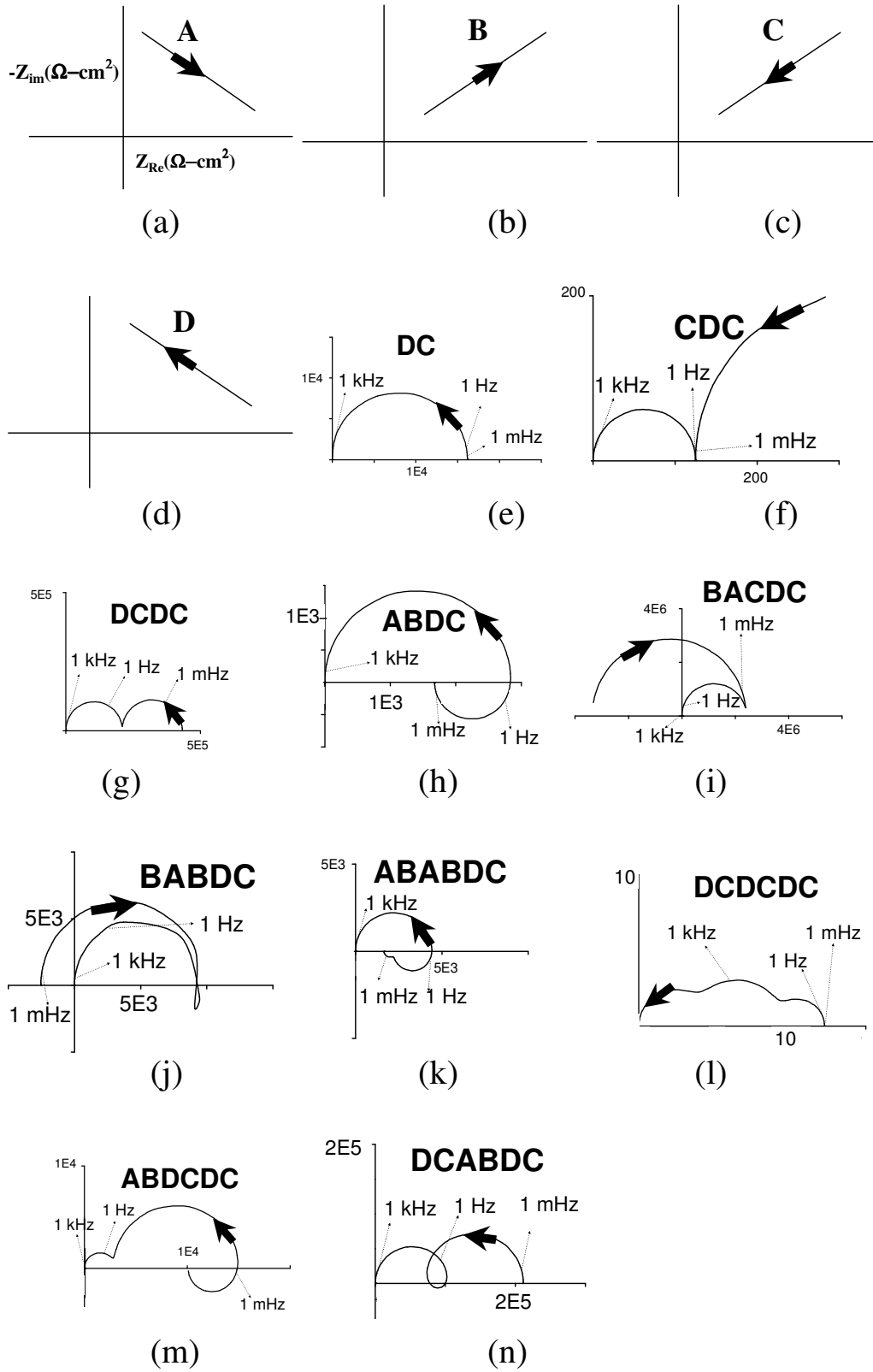
Table 1

Parameter	Minimum Value	Maximum Value	Number of steps	Increment type	Units
k_{10}	1e-12	1e-4	10	G	Moles-cm^{-2}s^{-1}
b_1	0	38	10	A	V^{-1}
k_{-10}	1e-12	1e-4	10	G	Moles-cm^{-2}s^{-1}
b_{-1}	-38	0	10	A	V^{-1}
k_{20}	1e-12	1e-4	10	G	Moles-cm^{-2}s^{-1}
b_2	0	38	10	A	V^{-1}
k_{30}	1e-12	1e-4	10	G	Moles-cm^{-2}s^{-1}
b_3	0	38	10	A	V^{-1}
C_{dl}	1e-6	1e-4	10	G	F-cm^{-2}
τ	1e-9	1e-4	10	G	Moles/cm^2
Overpotential V	0.05	2.05	10	A	voltage
Frequency (f)	1e-5	1e6	50	G	Hz

Table 2.

Mechanism	Constraint	DC	ABDC	DCDC	BACDC
1	(b1 > b2)	X	---	X	---
	(b1= b2)	X	---	---	---
	(b1 < b2)	X	X	---	---
2	(b1 > b2)	X	---	X	---
	(b1 = b2)	X	---	X	---
	(b1 < b2)	X	X	X	---
3	None	X	X	X	X
4, 5 and 6	(b1 > b2)	X	---	X	X
	(b1 = b2)	X	---	---	---
	(b1 < b2)	X	X	---	---
7	(b1 > b2)	X	X	X	---
	(b1 = b2)	X	---	---	---
	(b1 < b2)	X	X	X	---
8	(b1 > b2)	X	X	X	---
	(b1 = b2)	X	X	X	---
	(b1 < b2)	X	X	X	---
9 *	None	X	X	X	X